Scripta Materialia 130 (2017) 191–195

Contents lists available at ScienceDirect

Scripta Materialia

journal homepage: www.elsevier.com/locate/scriptamat

Regular article

A nanoindentation study of the viscoplastic behavior of pure lithium

Yikai Wang *, Yang-Tse Cheng

Department of Chemical and Materials Engineering, University of Kentucky, Lexington, KY 40506-0046, USA

ARTICLE INFO

Article history:
Received 11 November 2016
Received in revised form 5 December 2016
Accepted 5 December 2016
Available online xxxx

Keywords:
Lithium
Nanoindentation
Plasticity
Finite element analysis

ABSTRACT

Applying mechanical stresses is a possible approach to suppress dendrite and mossy lithium (Li) in Li metal electrodes. We conducted, in this work, nanoindentation tests on pure Li metal in an argon-filled glove box to study its viscoplastic behavior at room temperature. Both load-controlled and strain rate-controlled nanoindentations showed clear viscoplastic characteristics of Li. Based on an iterative finite element (FE) modeling approach, we determined a viscoplastic constitutive law for Li. In addition, we demonstrated by FE modeling that elastic modulus, on the order of GPas, has a negligible influence on the nanoindentation response of Li at ambient temperature.

With its high theoretical specific capacity (3862 mAh/g), lowest negative reduction potential (−3.040 V *vs.* the standard hydrogen electrode) and low density, Li metal has been considered to be a desirable negative electrode; thus triggered worldwide interest in the rechargeable Li metal batteries, such as Li-O_2 and Li-S batteries [1,2]. However, uncontrollable Li dendrites could penetrate through the separator and even the electrolyte, leading to short-circuit inside batteries. Mechanical suppression through polymer or solid state electrolytes (SSE) [3–5] and artificial stiffer solid electrolyte interphase (SEI) [6] has been proposed as an economical and promising solution for this problem. Based on the elastic deformation assumption, the theoretical work by Monroe et al. [3] indicated that SSE with a shear modulus twice of Li could inhibit Li dendrites. However, since the yield strength of Li is low, the stress generated at the separator/Li interface could cause plastic deformation of Li at a yield strength fraction of the modulus value [5,7,8]. Continued plastic deformation during repeated charging/discharging may cause Li redistribution, leading to shape change of Li at the anode/separator interface, and hence posing a threat to the safety and reliability of Li metal batteries [7,8]. A comprehensive understanding of the mechanical properties, especially the plastic flow behavior, of Li is necessary.

The mechanical test of Li metal is challenging because Li is extremely reactive with oxygen, nitrogen, water vapor, and carbon dioxide. Sample preparation and mechanical tests must be conducted in a protective environment. However, the few reported tensile [9], compression [10], and resonance tests [11] were not carried out in a protective atmosphere. Thus, it is unsurprising that the reported elastic modulus (E) ranges from 1.84 to 7.8 GPa, and the yield strength from 0.48 to 1.10 MPa [9–11]. Similar to other soft metals and alloys, such as Sn-alloys [12,13], indium [14] and lead [15], the deformation behavior of Li exhibits low yield strength and viscoplasticity. Because of the importance of viscoplastic behavior, we report, in this letter, nanoindentation measurements of Li performed in an argon-fill glove box. Combining FE modeling with nanoindentation measurements, we determined a constitutive law for viscoplastic deformation of Li during indentation loading. The influence of E on viscoplastic deformation was also studied.

High purity polycrystalline Li foils (99.9%, with thickness of 750 μm, Alfa Aesar) were used for nanoindentation measurements. Nanoindentation tests were conducted using the Nanoindenter G200 (Agilent) positioned inside an argon-filled glove box (both oxygen and moisture <0.1 ppm, MBRAUN) at 2.1 mbar (Fig. 1(a)). Load-controlled tests were carried out using a diamond Berkovich indenter (tip radius 200 nm) with loading rates, $\dot{F}$, ranging from 0.196 to 3.92 mN/s to the maximum load, F, of 5.88 mN. The holding periods were set to be 1 s. Constant strain rate-controlled tests were conducted with constant $\dot{F}/F$ values ranging from 0.1 to 1.0 s^{-1}. After nanoindentation measurements, the indents were examined by scanning electron microscope (SEM, FEI Quanta 250), as shown in Fig. 1(b). Since the maximum depth in each test was larger than 4500 nm, reproducible nanoindentation data were obtained despite of the slight surface roughness.

As shown in Fig. 1(c) and (d), the load-displacement (L-D) curves of Li exhibit obvious rate-dependent characteristics, i.e., the higher the loading rates, $\dot{F}$, the larger the load, F, is needed to reach the same indentation depth. For constant strain rate-controlled nanoindentation tests, the load corresponding to the same depth increases with the value of $\dot{F}/F$. The creep penetration depth during the holding period increases with the loading rate. Similar to viscoelastic materials [16], "noses" appeared at the initial part of the unloading curves. The elastic recovery during

* Corresponding author.
E-mail address: ywa286@g.uky.edu (Y. Wang).

http://dx.doi.org/10.1016/j.scriptamat.2016.12.006

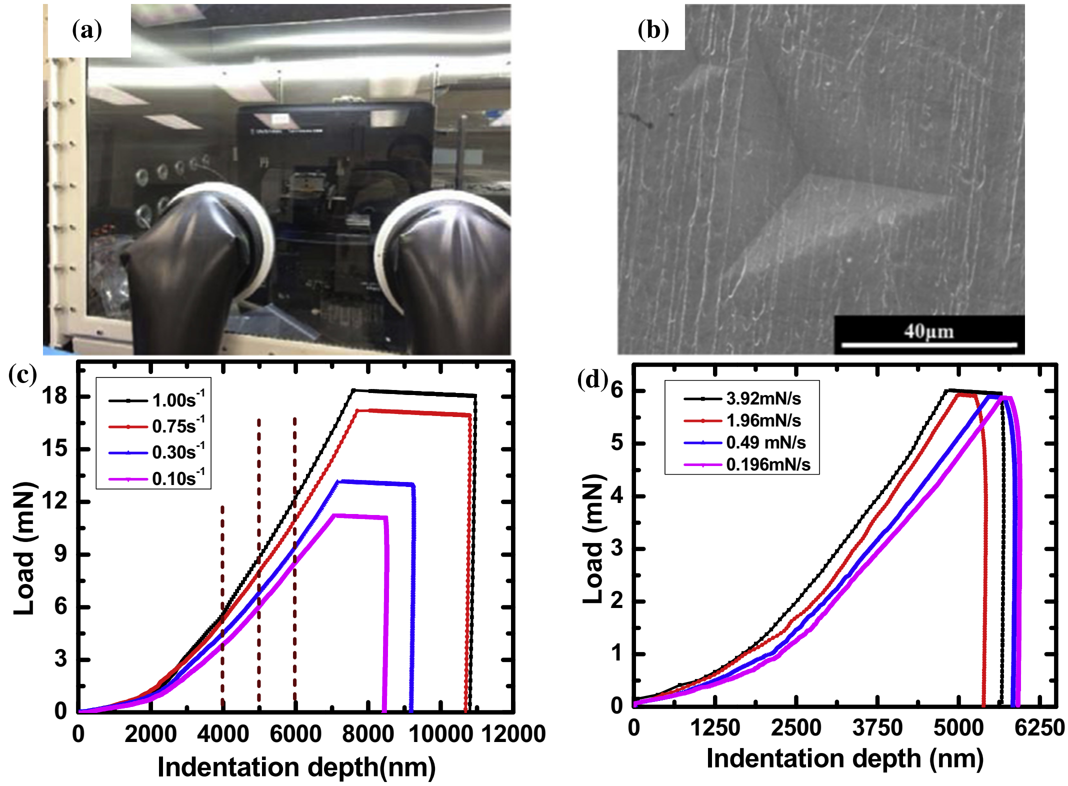

Fig. 1. (a) The G200 nanoindentation system in the Ar-filled glove box; (b) a typical SEM image of the indent on the Li foil; (c) typical L-D curves with different values of $\dot{F}/F$; and (d) typical L-D curves with different loading rates.

the unloading is only few tens of nanometers. Therefore, the indentation deformation is mainly plastic. In the following analysis, we focus on the loading part as our interest is the constitutive law of viscoplasticity.

The rate-dependent plasticity, or viscoplasticity, of Li during the indentation loading may originate from two mechanisms. First, the thermally activated diffusion and viscous flow [17], such as Nabarro-Herring creep, Coble creep and dislocation climb, are expected to occur since the homologous temperature, T_{rm}/T_{melt}, is 0.66 at room temperature for Li. Second, the stable crystal structure of Li is body centered cubic (BCC) at room temperature [18]. The plastic deformation of BCC metals and alloys is governed by the motion of screw dislocations via kink pairs which require thermal activation [19,20]. Therefore, the viscoplasticity of Li is likely the result of those multiple physical mechanisms. Although a mechanism-based model would have been more reliable in describing the viscoplastic behavior of Li, such a model would require detailed information at the atomic scale (e.g., dislocation structure and diffusion coefficient) that is generally unavailable. Instead, several empirical or phenomenological constitutive models, such as Anand model [21,22], Johnson-Cook model [23], and Perzyna model [24,25], have been developed based on somewhat different assumptions to describe viscoplastic deformation of soft metals and alloys [13,14,26,27]. Anand model does not have an explicit yield condition or loading/unloading criterion, such that plastic strain can take place under any nonzero stress. This model is preferred for the steady-state creep under constant load or stress [13,14]. Johnson-Cook model has been widely used for various materials over a wide range of temperature and strain rate, especially for high strain rate deformation. But consistent parameters could not be obtained for Li with Johnson-Cook model (see Fig. S1 and Table SI in the Supplementary material). The one-dimension Perzyna model and Cowper-Symonds model [28] have the equivalent functional form. Cowper-Symonds model was derived for high rate impact tests of cantilever beams, and thus suitable for high strain rate deformation; while Perzyna model was derived for general elastic-viscoplastic solids under general stress states [24,25]. It has a

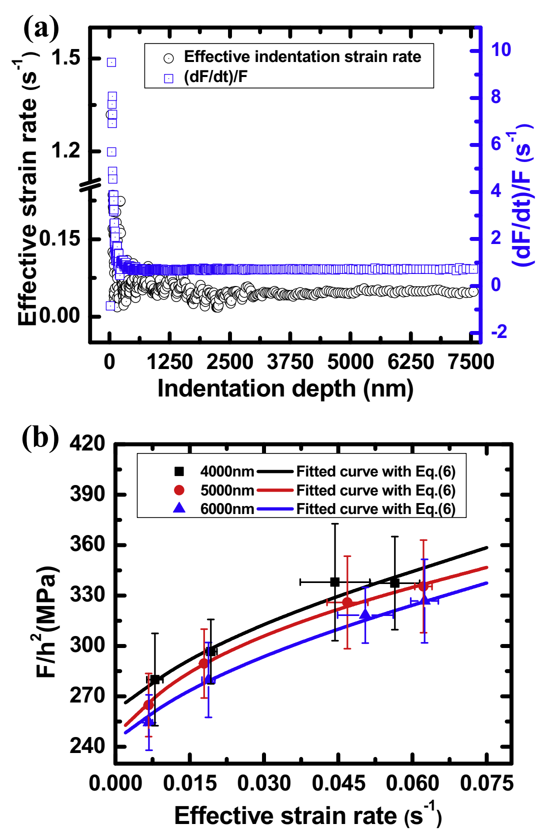

Fig. 2. (a) The variation of effective indentation strain rate $(0.12\dot{h}/h)$ and $\dot{F}/F$ with indentation depth ($\dot{F}/F$ is $0.75s^{-1}$ in the experimental). Prior to 3500 nm, the distribution of strain rate is scattering. The effective strain rate trends to be a constant value only after 3500 nm. (b) The $F/h^2 vs. \dot{\varepsilon}_{ef}$ relationship corresponding to different indentation depths. The averaged values of F/h^2 and the effective strain rates $(0.12\dot{h}/h)$ were used here.